Journal of Alloys and Compounds 480 (2009) 587–591

Contents lists available at ScienceDirect

Journal of Alloys and Compounds

journal homepage: www.elsevier.com/locate/jallcom

Phase transition and thermodynamic properties of MgTe under high pressure

Hongzhi Fu[a,*], WenFang Liu[b], Feng Peng[a], Tao Gao[c]

[a] College of Physics and Electronic Information, Luoyang Normal College, Luoyang 471022, People's Republic of China
[b] College of Chemistry and Chemical Engineering, Luoyang Normal College, Chengdu 610065, People's Republic of China
[c] Institute of Atomic and Molecular Physics, Sichuan University, Chengdu 610065, People's Republic of China

ARTICLE INFO

Article history:
Received 24 May 2008
Received in revised form 22 January 2009
Accepted 1 February 2009
Available online 10 February 2009

PACS:
62.20.de
64.70.Kb
71.15.Mb

Keywords:
MgTe
Phase transitions
Thermodynamic properties

ABSTRACT

The transition phase of MgTe from rock salt structure (B1) to cesium chloride structure (B2) is investigated by *ab initio* plane-wave pseudopotential density functional theory method. The thermodynamic properties of the B1 and B2 structures are obtained through the quasi-harmonic Debye model. Our results indicated that MgTe undergoes a structural phase transition from B1 to B2 at about 90.32 GPa. The dependences of the relative volume V/V_0 on the pressure P, the Debye temperature Θ and heat capacity C_V on the pressure P, the Grüneisen parameter ratio $(\gamma - \gamma_0)/\gamma_0$ on pressure P, the bulk moduli ratio $(B - B_0)/B_0$ on pressure P, as well as the heat capacity C_V on the temperature T are estimated.

1. Introduction

With the wide-gap binary $A^N B^{8-N}$ semiconductors and promising potential of alkaline earth chalcogenides (AECs) used for various electrical and optical devices, MgTe has recently led to extensive studies in both theoretical [1–7] and experimental [8,9]. Recently, lots of properties of solids have become possible to compute with great accuracy from the first principles methods. These calculations are therefore used to investigate the structures of materials at high pressures. The significant advances in computational materials science have made possible the use of *ab initio* quantum mechanical techniques to predict MgTe the electronic structure [3,6], the phase transition [4,5] and optical properties [7]. Such studies could play a significant role from the standpoint of predicting the performance of the material under extreme conditions.

Despite much theoretical works, the MgTe is so far not well understood for some of its properties, for example, the effect of pressure on its thermodynamic properties. This has motivated us to examine the structural and thermodynamic properties of MgTe, with emphasis on their dependence on hydrostatic pressure. Till today, these properties remain as a source for investigation and for possible new discoveries. In the present paper, the rock salt structure (B1) to cesium chloride structure (B2) transition volumes and pressures were deduced, and the structural and thermodynamic properties of MgTe (the B1 and B2 phases) were investigated.

2. Computational approach

Through the Cambridge Serial Total Energy Package (CASTEP) program [10] and the quasi-harmonic Debye model [11], all calculations are performed based on the plane-wave pseudopotential density function theory (DFT) [12,13]. Vanderbilt-type ultrasoft pseudopotentials (USPP) [14] are employed to describe the electron–ion interactions. The effects of exchange correlation interaction are treated with the generalized gradient approximation (GGA) of Perdew–Burke–Eruzerhof (PBE) [15]. In the structure calculation, a plane-wave basis set with energy cut-off 360.00 eV is used. Pseudo-atomic calculations are performed for $Mg3s^2$ and $Te5s^25p^4$. For the Brillouin-zone sampling, we adopt the $6 \times 6 \times 6$ Monkhorst–Pack mesh [16], where the self-consistent convergence of the total energy is at 10^{-7} eV/atom and the maximum force on the atom is below 10^{-5} eV/Å.

3. Results and discussions

Within *ab initio* calculations, the structural properties are very important first step to understand the material properties from a

* Corresponding author. Tel.: +86 379 65515016; fax: +86 379 65515016.
E-mail address: fhzscdx@163.com (H. Fu).

0925-8388/$ – see front matter © 2009 Elsevier B.V. All rights reserved.
doi:10.1016/j.jallcom.2009.02.009

Table 1
The lattice constants (Å), bulk modulus (GPa) and its pressure derivation, elastic constants C_{ij} (GPa) of the B1 and B2 structures of MgTe at $P=0$ and $T=0$, together with the transition pressures P_t (GPa).

This work	Other theoretical calculations	Experiments
B1 structure		
a 5.947	5.86 [7], 5.84 [4], 5.9242 [5], 5.8548 [28]	
B_0 47.87	52 [7], 53.3 [4], 54.5 [5], 48.6 [28]	
B_0' 3.78	4.1 [7], 4.04 [5], 3.88 [28]	
C_{11} 89.66	185.36 [19], 96.3 [22], 124.2 [23], 82.8 [7]	
C_{12} 32.66	29.88 [19], 17.6 [22], 65.9 [23], 25.7 [7]	
C_{44} 26.97	31.86 [19], 10.2 [22], 65.9 [23], 38.9 [7]	
P_t 90.32	68.2 [19], 69.6 [20], 176 [22], >60 [24], 69.7 [25], 190.8 [26], 101.8 [27], 69.6 [5]	>60 [21]
B2 structure		
a 3.6982	3.6238 [18], 3.6826 [5], 3.6544 [6], 3.6826 [5]	
B_0 45.68	52.348 [18], 49.5 [5], 53.22 [6], 49.5 [5]	
B_0' 3.582	3.913 [18], 4.20 [5], 4.20 [5]	
C_{11} 82.2	53.54 [18]	
C_{12} 32.8	51.6 [18]	
C_{44} 7.5	1.6 [18]	

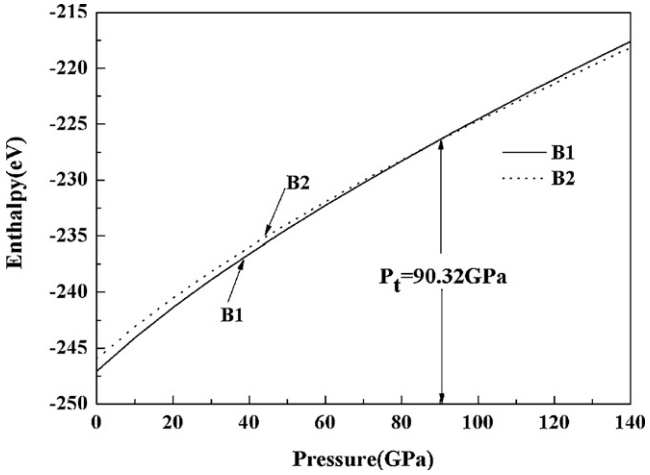

Fig. 2. Enthalpy as a function of pressure for MgTe.

microscopic point of view. The calculated equilibrium lattice constants a, elastic constants C_{ij}, zero-pressure bulk modulus B_0 and its pressure derivation B_0' from the Birch–Murnaghan equation of state (EOS) [17] are listed in Table 1, together with other theoretical results [5–7,18–27,4] and the experimental data [28]. The agreements among them are good. The calculations of elastic constants C_{ij} are shown in Appendix A.

As known, there are two basic methods to obtain the zero-temperature pressure of transition for MgTe. The first one is the slope of the common tangent of both E–V curves in Fig. 1. The second one is enthalpy, $H=E+PV$, i.e., at the phase transition pressure P, the enthalpies of B1 and B2 structures attaining the same. The enthalpy H as a function of pressure P is illustrated in Fig. 2. The calculated transition pressure (B1 to B2) $P_t=90.32$ GPa, is about 24.5% greater than the one predicted by Narayana et al. [20], about 52.7% smaller than the one calculated by Cervantes et al. [25] and very close to that of Rabah et al. [26].

The EOS of MgTe in both B1 and B2 phases are obtained using the quasi-harmonic Debye model [11]. We illustrate the normalized primitive cell volume V/V_0 (V_0 is the zero-pressure equilibrium primitive cell volume) dependences on pressure P at $T=300$ and 2000 K in Fig. 3. Obviously, when temperature increases, the curve of V/V_0-P becomes steeper, indicating that MgTe is compressed much more easily at higher temperature. At transition pressure P_t, our calculation shows that there is no noticeable volume change between B1 and B2 phases as given in Fig. 3. This likely indicates that transition is second order. The volume (B1 to B2) reduces 6.11% and 5.85% at $T=300$ and 2000 K, respectively.

Elastic constants are believed to be related to the strength of materials. To investigate the hardness of materials, the bulk and shear moduli are frequently calculated. The elastic constants determine the response of the crystal to the external forces and play an important part in determining the strength of the materials [29]. Values of these elastic constants provide valuable information about the bonding characteristic between the adjacent atomic planes and the anisotropic character of the bonding and structural stability. On compression, at $T=300$ and 2000 K, the pressure-dependence of bulk moduli ratios of MgTe in both B1 and B2 structures, $(B-B_0)/B_0$ (B_0 is the zero-pressure bulk modulus), are plotted in Fig. 4. We see that the bulk modulus, a property of a material which defines its resistance to volume change when compressed, increases as a function of the hydrostatic pressure in both B1 and B2 phases. This behavior is common to all II–VI compounds. It shows the fact that the effect of increasing pressure on MgTe is the same as increasing its temperature.

The Grüneisen parameter γ is thought to be described the alteration in a crystal lattice's vibration's frequency based on the lattice's increase or decrease in volume as a result of temperature change. It is directly related to the EOS. The calculations of Grüneisen parameter γ is shown in Appendix A. We have determined the

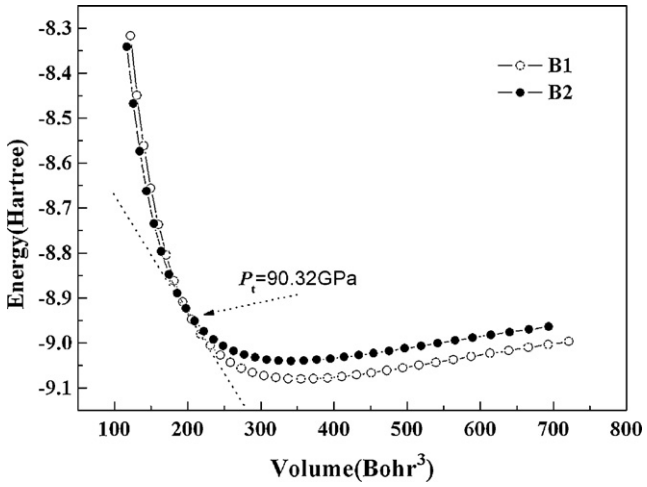

Fig. 1. Energy as a function of primitive cell volume for MgTe.

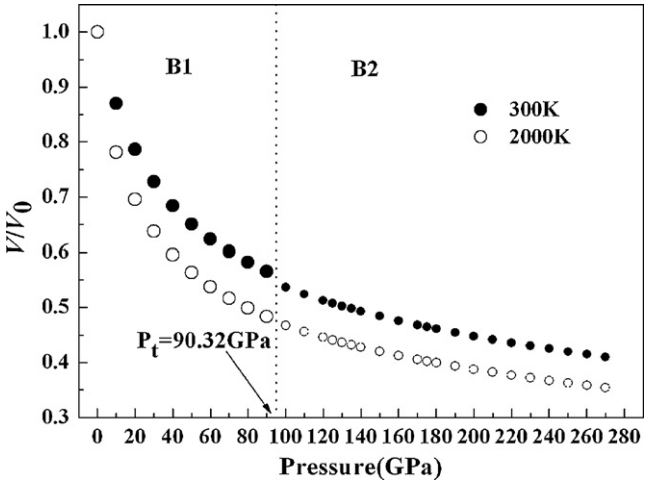

Fig. 3. The normalized volume–pressure diagram of the B1 and B2 structures for MgTe at 200 and 2000 K temperatures.

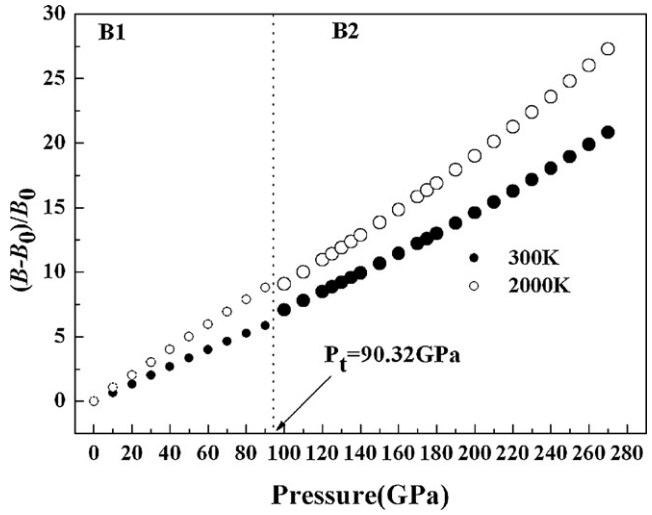

Fig. 4. The bulk modulus ratios–pressure of the B1 and B2 structures for MgTe at 300 and 2000 K temperatures.

pressure-dependence of Grüneisen parameter γ for both the phases B1 and B2, which are shown in Fig. 5. Below the phase transition pressure P_t, the Grüneisen parameter ratios (B1 phase), $(\gamma-\gamma_0)/\gamma_0$, increase (not linear) with the pressure. However, above the phase transition pressure P_t, the Grüneisen parameter ratios (B2 phase), $(\gamma-\gamma_0)/\gamma_0$, increase (nearly linear) with the pressure. When the pressure is near P_t, the ratios of the B1 and B2 phases, $(\gamma-\gamma_0)/\gamma_0$, jump up by 7.68% and 7.07% at the temperature 300 and 2000 K, respectively.

The variations of the Debye temperature Θ and the heat capacity C_V with pressure P for the B1 and the B2 structures of MgTe are shown in Fig. 6. They are normalized by $(X-X_0)/X_0$, where X and X_0 are the Debye temperature or heat capacity at any pressure P and zero pressure. The calculations of Debye temperature Θ and the heat capacity C_V are shown in Appendix A. It is shown that, for the two phases of MgTe, when the temperature keeps constant, the Debye temperature Θ increases almost linearly with applied pressures. The Debye temperatures Θ of the B1 and the B2 structures at the temperature of 2000 K are higher than those at 300 K, as shows the fact that the vibration frequency of the particles in MgTe changes with the pressures and the temperatures. On the other hand, the heat capacity C_V decreases with the applied pressures. In Fig. 7, the heat capacity of the B1 and B2 structures of MgTe

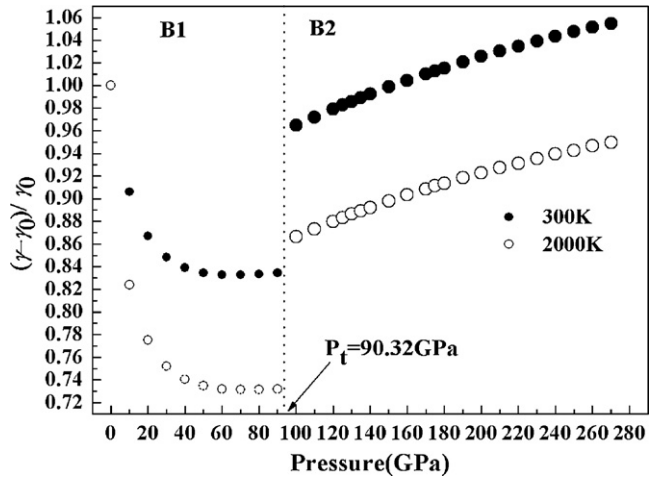

Fig. 5. The Grüneisen parameter ratios–pressure of the B1 and B2 structures for MgTe at 300 and 2000 K temperatures.

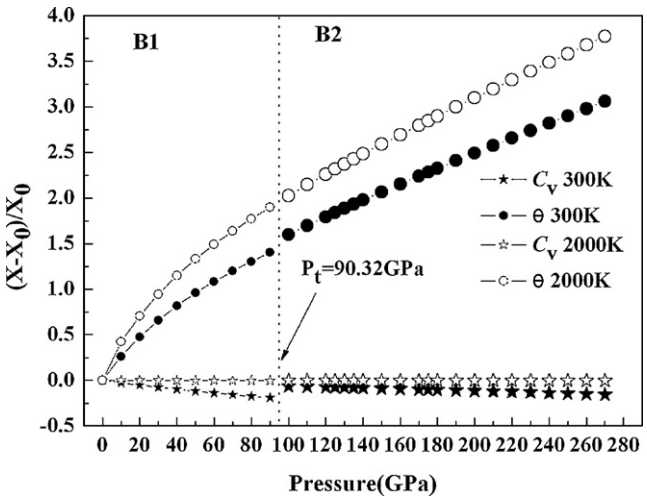

Fig. 6. Variation of thermodynamic parameters X (X: Debye temperature or heat capacity) with pressure P. They are normalized by $(X-X_0)/X_0$, where X and X_0 are the Debye temperature or heat capacity at any pressure P and zero pressure at the temperatures of 300 and 2000 K.

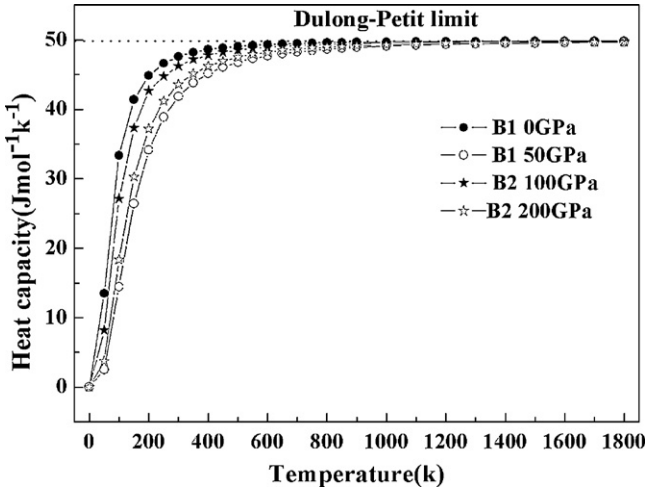

Fig. 7. The heat capacity of the B1 and B2 structures of MgTe at various pressures and temperatures.

are plotted for several pressures. It is shown that when $T<1400$ K, the heat capacity C_V is dependent on both the temperature T and the pressure P. This is due to the anharmonic approximations of the Debye model. However, at higher pressures and/or higher temperatures, the anharmonic effect on C_V is suppressed, and C_V is very close to the Dulong–Petit limit.

4. Conclusions

We have investigated the transition phase of MgTe from the B1 structure to the B2 structure by the *ab initio* plane-wave pseudopotential density functional theory method using package CASTEP. It is found that the transition phase from the B1 to B2 occurs at 90.32 GPa according to the usual condition of equal enthalpy. Through the quasi-harmonic Debye model, we have successfully obtained the dependences of the relative volume V/V_0 on the pressure P, the Debye temperature Θ and heat capacity C_V on the pressure P, the Grüneisen parameter ratio $(\gamma-\gamma_0)/\gamma_0$ on pressure P, bulk moduli ratio $(B-B_0)/B_0$ on pressure P and the heat capacity C_V on the temperature T.

Acknowledgments

This project was supported by the National Natural Science Foundation of China under grant no. 40804034, and by the Natural Science Foundation of the Education Department of Henan province of China under grant no. 20020610001.

Appendix A

A.1. Calculations of MgTe elastic constants, bulk modulus, etc.

On the basis of the Hooke's law, the elastic stiffness tensor C_{ijkl} can be expressed as [30,31]

$$C_{ijkl} = \left(\frac{\partial \sigma_{ij}(x)}{\partial e_{kl}}\right) X \tag{1}$$

where σ_{ij} and e_{kl} are the applied stress and Eulerian strain tensors and X and x are the coordinates before and after the deformation. Under the hydrostatic pressure P, the C_{ijkl} can be given by [31,32]

$$C_{ijkl} = \left(\frac{1}{V(x)}\frac{\partial^2 E(x)}{\partial e_{i_j}\partial e_{kl}}\right)_X + \frac{P}{2}(2\delta_{ij}\delta_{kl} - \delta_{ik}\delta_{jl} - \delta_{il}\delta_{jk}) \tag{2}$$

where δ is the finite strain variable.

For the case of isotropic stress, the three nonindependent elastic constants of cubic crystals (C_{11}, C_{12}, and C_{44}) are calculated by the second derivatives of the total energy density with respect to the infinitesimal strain tensor e_{kl}. The strain

$$e = \begin{pmatrix} \delta & 0 & 0 \\ 0 & 0 & 0 \\ 0 & 0 & 0 \end{pmatrix} \tag{3}$$

is adopted to each V for the calculation of C_{11}. Then

$$C_{11} = \frac{1}{V}\frac{\partial^2 E}{\partial \delta^2}_{|\delta=0} \tag{4}$$

The e_{kl} matrix for the calculation of C_{44} is

$$e = \begin{pmatrix} 0 & \delta & \delta \\ \delta & 0 & \delta \\ \delta & \delta & 0 \end{pmatrix} \tag{5}$$

Then

$$C_{44} = \frac{1}{12V}\frac{\partial^2 E}{\partial \delta^2}_{|\delta=0} \tag{6}$$

C_{12} is calculated from C_{11} and $C_{11} - C_{12}$, The e_{kl} matrix for the calculation of $C_{11} - C_{12}$ is

$$e = \begin{pmatrix} \delta & 0 & 0 \\ 0 & -\delta & 0 \\ 0 & 0 & 0 \end{pmatrix} \tag{7}$$

Then

$$C_{11} - C_{12} = \frac{1}{2V}\frac{\partial^2 E}{\partial \delta^2}_{|\delta=0} \tag{8}$$

The pressure P versus the normalized volume V_n is obtained through the following thermodynamic relationship [33]:

$$P = -\frac{dE}{dV} = \frac{B_0}{B_0'}[V_n^{-B_0'} - 1] \tag{9}$$

where $B_0' = dB_0/dp$ and B_0 are the pressure derivative of the bulk modulus and zero-pressure bulk modulus, respectively.

For the specific case of the cubic lattices, the shear modulus G, the Young's modulus E, Poisson's ratio σ and anisotropy factor (A) [34], for an isotropic material are given by

$$G = \frac{1}{2}(G_V + G_R) \tag{10}$$

$$E = \frac{9BG}{3B + G} \tag{11}$$

$$\sigma = \frac{3B - 2G}{2(3B + G)} = \frac{C_{12}}{C_{11} + C_{12}} \tag{12}$$

$$A = \frac{2C_{44} + C_{12}}{C_{11}} \tag{13}$$

respectively.

Where $G_V = (2C' + 3C_{44})/5$, $G_R = 15(6/C' + 9/C_{44})^{-1}$, $C' = (C_{11} - C_{12})/2$. G_V and G_R are the Voigt shear modulus and the Reuss shear modulus, respectively.

A.2. Calculations of thermodynamic properties of MgTe

To investigate the thermodynamic properties of MgTe, we here apply the quasi-harmonic Debye model [11], in which the non-equilibrium Gibbs function $G^*(V; P, T)$ takes the form of

$$G^*(V; P, T) = E(V) + PV + A_{Vib}(\theta(V); T) \tag{14}$$

where $E(V)$ is the total energy per unit cell for γ-MgTe, $\theta(V)$ is the Debye temperature, and the vibrational Helmholtz free energy A_{Vib} can be written as [35,36]

$$A_{Vib}(\theta; T) = nKT \times \left[\frac{9}{8}\frac{\theta}{T} + 3\ \ln(1 - e^{-\theta/T}) - D\left(\frac{\theta}{T}\right)\right] \tag{15}$$

where $D(\theta/T)$ represents the Debye integral and n is the number of atoms per formula unit. θ is expressed by [36],

$$\theta = \frac{\hbar}{K}[6\pi^2 V^{1/2}]^{1/3} f(\sigma)\sqrt{\frac{B_S}{M}} \tag{16}$$

where M is the molecular mass per formula unit, B_S is the adiabatic bulk modulus approximated by the static compressibility [11]

$$B_S \approx B(V) = V\left(\frac{d^2 E(V)}{dV^2}\right) \tag{17}$$

and $f(\sigma)$ is given by Refs. [37,38].

Therefore, the nonequilibrium Gibbs function $G^*(V; P, T)$ as a function of $(V; P, T)$ can be minimized with respect to volume V as

$$\left(\frac{\partial G^*(V; P, T)}{\partial V}\right)_{P,T} = 0. \tag{18}$$

By solving Eq. (18), one can get the thermal EOS $V(P, T)$. The isothermal bulk modulus B_T is given by [11]

$$B_T(P, T) = V\left(\frac{\partial^2 G^*(V; P, T)}{\partial V^2}\right)_{P,T} \tag{19}$$

The heat capacity C_V and the thermal expansion (α) are expressed as

$$C_V = 3nK\left[4D\left(\frac{\theta}{T}\right) - \frac{3\theta/T}{e^{\theta/T} - 1}\right] \tag{20}$$

$$\alpha = \frac{\gamma C_V}{B_T V} \tag{21}$$

where γ is the Grüneisen parameter defined as

$$\gamma = -\frac{d\ \ln\theta(V)}{d\ln V} \tag{22}$$

References

[1] W. Zachariasen, Z. Phys. Chem. Stoechiom. Verwandtschaftsl. 128 (1927) 417.
[2] W. Klemm, K. Wahl, Z. Anorg, Allg. Chem. 266 (1951) 289.
[3] C.Y. Yeh, Z.W. Lu, S. Froyen, A. Zunger, Phys. Rev. B 46 (1992) 10086.
[4] P.E. Van Camp, V.E. Van Doren, Int. J. Quant. Chem. 55 (1995) 339.
[5] P.E. Van Camp, V.E. Van Doren, J.L. Martins, Phys. Rev. B 55 (1997) 775.
[6] C.B. Chaudhuri, G. Pari, A. Mookerjee, Phys. Rev. B 60 (1999) 11846.
[7] F. Drief, A. Tadjer, D. Mesri, H. Aourag, Catal. Today 89 (2004) 343.
[8] A. Kuhn, A. Chevy, M.J. Naud, J. Cryst. Growth 9 (1961) 263.
[9] S.G. Parker, A.R. Reinberg, J.E. Pinnel, W.C. Holton, J. Electrochem. Soc. 118 (1971) 979.
[10] V. Milman, B. Winkler, J.A. White, C.J. Packard, M.C. Payne, E.V. Akhmatskaya, R.H. Nobes, Int. J. Quant. Chem. 77 (2000) 895.
[11] M.A. Blanco, E. Francisco, V. Luana, Comput. Phys. Commun. 158 (2004) 57.
[12] P. Hohenberg, W. Kohn, Phys. Rev. B 136 (1964) 384.
[13] W. Kohn, L.J. Sham, Phys. Rev. A 140 (1965) 1133.
[14] D. Vanderbilt, Phys. Rev. B 41 (1990) 7892.
[15] J.P. Perdew, K. Burke, M. Ernzerhof, Phys. Rev. Lett. 77 (1996) 3865.
[16] H.J. Monkhorst, J.D. Pack, Phys. Rev. B 13 (1976) 5188.
[17] F.D. Murnaghan, Proc. Natl. Acad. Sci. U.S.A. 30 (1994) 244.
[18] D. Rached, M. Rabah, R. Khenata, N. Benkhettou, H. Baltache, M. Maachou, M. Ameri, J. Phys. Chem. Solids 67 (2006) 1668.
[19] P. Bhardwaj, S. Singh, N.K. Gaur, Turk. J. Phys. 32 (2008) 1.
[20] C. Narayana, V.J. Nesamony, A.L. Ruoff, Phys. Rev. B 56 (1997) 14338.
[21] D. Varshney, N. Kaurav, U. Sharma, R.K. Singh, J. Phys. Chem. Solids 69 (2008) 60.
[22] G.K. Straub, W.A. Harrison, Phys. Rev. B 39 (1989) 10325.
[23] T.S. Duffy, R.J. Hemley, H. Mao, Phys. Rev. Lett. 74 (1995) 1371.
[24] A.L. Ruoff, T. Li, A.C. Ho, M.F. Pai, R.G. Greene, C. Narayana, J.C. Molstad, S.S. Trail, F.J. DiSalvo Jr., P.E. van Camp, Phys. Rev. Lett. 81 (1998) 2723.
[25] P. Cervantes, Q. Williams, M. Cote, M. Rohlfing, M.L. Cohen, S.G. Louie, Phys. Rev. B 58 (1998) 9793.
[26] M. Rabah, D. Rached, M. Benkhettou, R. Khenata, H. Baltache, B. Soudini, M. Ameri, H. Abid, Comput. Mater. Sci. 37 (2006) 603.
[27] B. Freytag, J. Phys. Condens. Matter 6 (1994) 9875.
[28] T. Li, H. Luo, R.G. Greene, A.L. Ruoff, S.S. Trail, F.J. Disalvo, Phys. Rev. Lett. 74 (1995) 5232.
[29] P. Ravindran, L. Fast, P.A. Korhavyi, B. Johansson, J. Wills, O. Eriksson, J. Appl. Phys. 84 (1998) 4891.
[30] J.F. Nye, Physical Properties of Crystals, Clarendon Press, Oxford, 1985.
[31] B.B. Karki, G.J. Ackland, J. Crain, J. Phys. Condens. Matter 9 (1997) 8579.
[32] J.H. Wang, J. Li, S. Yip, S. Phillpot, D. Wolf, Phys. Rev. B 52 (1995) 12627.
[33] L. Fast, J.M. Wills, B. Johansson, O. Eriksson, Phys. Rev. B 51 (1995) 17431.
[34] D. Iotova, N. Kioussis, S.P. Lim, Phys. Rev. B 54 (1996) 14413.
[35] M.A. Blanco, A. Martín Pendás, E. Francisco, J.M. Recio, R. Franco, J. Mol. Struct. (Theochem.) 368 (1996) 245.
[36] M. Flárez, J.M. Recio, E. Francisco, M.A. Blanco, A. Martín Pendás, Phys. Rev. B 66 (2002) 144112.
[37] E. Francisco, J.M. Recio, M.A. Blanco, A. Martín Pendás, A. Costales, J. Phys. Chem. 102 (1998) 1595.
[38] E. Francisco, M.A. Blanco, G. Sanjurjo, Phys. Rev. B 63 (2001) 094107.